Overdoped metals in the $Tl_2Ba_2CuO_{6+\delta}$ and $TlSr_2CaCu_2O_{7-\delta}$ systems

Y. Shimakawa
Materials Science Division and Science and Technology Center for Superconductivity, Argonne National Laboratory, Argonne, Illinois 60439
and Fundamental Research Laboratories, NEC Corporation, 34 Miyukigaoka, Tsukuba 305, Japan

J. D. Jorgensen
Materials Science Division and Science and Technology Center for Superconductivity, Argonne National Laboratory, Argonne, Illinois 60439

T. Manako and Y. Kubo
Fundamental Research Laboratories, NEC Corporation, 34 Miyukigaoka, Tsukuba 305, Japan
(Received 20 July 1994)

We have synthesized overdoped metallic samples of $Tl_2Ba_2CuO_{6+\delta}$ and $TlSr_2CaCu_2O_{7-\delta}$ beyond the superconductor-metal phase boundary by annealing the samples in high-pressure oxygen. Oxygen incorporation is clearly demonstrated by structural refinements of neutron powder-diffraction data and reversible changes in sample weight. The same $\sim T^2$ scattering mechanism in transport properties as previously observed in superconducting samples is observed in the present overdoped metallic samples. Hall coefficients do not change sign and are still positive for the overdoped metals. Although the crystal structures of both compounds change gradually and continuously with oxygen doping beyond the superconductor-metal phase boundary, the electronic structure of the "further overdoped metals" might still be near the supeconductor-metal phase boundary.

I. INTRODUCTION

In the phase diagram of high-T_c superconductors as a function of carrier doping, superconductivity occurs in an intermediate region between an antiferromagnetic insulator and a metal. This feature suggests that the high-T_c superconductivity is connected with a state described as either a spin liquid or a Fermi liquid. Therefore, in order to formulate a mechanism of high-T_c superconductivity, studies of both extremes of behavior are important. However, there are few examples of overdoped materials, so research on overdoped compounds has been somewhat limited.

Heavily Sr or Ba-doped La_2CuO_4 is the best-known example of an overdoped compound. In the $(La_{1-x}Sr_x)_2CuO_4$ system, the superconducting transition temperature (T_c) decreases in the overdoped region ($x > 0.075$) and the superconductivity disappears around $x = 0.15$. The most remarkable feature is that the Hall coefficient changes its sign from positive to negative near $x = 0.15$, the superconductor-metal phase boundary. This suggests a singularity near the superconductor-metal phase boundary and a drastic change in the electronic structure.[1] In the $(La_{1-x}Sr_x)_2CuO_4$ system, a phase transition from orthorhombic to tetragonal symmetry[2–4] complicates understanding the intrinsic properties in the overdoped region.

Other examples of overdoped compounds are $Tl_2Ba_2CuO_{6+\delta}$ (Refs. 5 and 6) and $TlSr_2CaCu_2O_{7-\delta}$,[7] both of which show typical behavior, such as decreasing T_c with increasing hole-carrier concentration, in the overdoped region. In these compounds, oxygen nonstoichiometries in the TlO layers control the carrier concentration. Samples synthesized in 1 atm oxygen show metallic conductivity to below liquid-He temperature and reduction in an argon atmosphere gives rise to superconductivity up to 85 K ($Tl_2Ba_2CuO_{6+\delta}$) and 75 K ($TlSr_2CaCu_2O_{7-\delta}$). No evidence of inhomogeneity is observed in studies of the superconductivity or crystal structure for the overdoped Tl materials. In contrast to $(La_{1-x}Sr_x)_2CuO_4$, the Hall coefficients and the spin susceptibilities for both compounds show gradual and continuous changes as the behavior changes from superconductors to metals by varying the composition. There seems to be no singularity at the superconductor-metal phase boundary, suggesting that the electronic structures for the superconducting and the metallic states are quite similar.[6,7]

Although previous studies of transport properties for overdoped Tl compounds suggested a similarity of the electronic structure of the superconducting and metallic states, the continuity at the superconductor-metal phase boundary is still a little vague because the $Tl_2Ba_2CuO_{6+\delta}$ and $TlSr_2CaCu_2O_{7-\delta}$ samples annealed in 1 atm oxygen, which show metallic conductivity to below liquid-He temperature, seem to lie very close to the superconductor-metal phase boundary. The release of very small amounts of oxygen from these metallic samples causes superconductivity.[5,7] Thus, in order to confirm the continuity of the electronic structure, we sought to obtain metallic samples doped further beyond the superconductor-metal phase boundary. Changes in

the crystal structures and the physical properties at crossing the superconductor-metal phase boundary gives important information about the continuity of the electronic structure. It is also important to learn whether the Hall coefficient changes its sign in the overdoped region beyond the boundary.

Recently, a striking feature in the normal state (above T_c) transport properties of high-T_c superconductors has been observed: T^2 dependence of the inverse Hall mobility $\mu_H^{-1}=\rho/R_H$ (or Hall angle, $\cot\theta_H=\mu_H^{-1}/B$). This simple relationship is observed in a variety of samples over a broad range of compositions extending from the underdoped through the optimally doped to the overdoped states.[8-16] Kubo and Manako[14] reported a clear T^2 dependence of the inverse Hall mobility for overdoped $Tl_2Ba_2CuO_{6+\delta}$ and $TlSr_2CaCu_2O_{7-\delta}$ samples and claimed that the scattering mechanism in transport properties was consistent with a Fermi-liquid description.[14] This relationship provides a test for examining the continuity of the electronic structure at the superconductor-metal phase boundary.

In this study, we have succeeded in obtaining overdoped metallic samples beyond the superconductor-metal phase boundary by annealing the samples in high-pressure oxygen. The incorporated oxygen atoms are clearly seen in structural refinements using neutron powder-diffraction data and in reversible weight changes. This paper reports the crystal structures, resistivities, and Hall coefficients in the overdoped metallic $Tl_2Ba_2CuO_{6+\delta}$ and $TlSr_2CaCu_2O_{7-\delta}$ samples, and discusses the continuity of these quantities at the superconductor-metal phase boundary. The electronic structures of both superconducting and metallic states are also discussed in the light of the T^2 dependence of the inverse Hall mobility.

II. SYNTHESIS AND DATA COLLECTION

Powder samples of $Tl_2Ba_2CuO_{6+\delta}$ and $TlSr_2CaCu_2O_{7-\delta}$ were synthesized using the same methods described in previous papers.[7,17] $Tl_2Ba_2CuO_{6+\delta}$ has been reported to show two structural symmetries; tetragonal or orthorhombic.[17] Tetragonal samples were used in this study. Initially all samples were annealed in 1 atm oxygen at 350 °C for 10 h to obtain homogeneous oxygen distributions. These samples were confirmed to be nonsuperconducting. Then, the samples were annealed in high-pressure oxygen to obtain higher doping levels by introducing more oxygen into the samples. This process was performed by annealing the samples at 200–400 atm oxygen (using a mixture of 20% oxygen and 80% argon) at 300–350 °C for 5 h by using a KOBELCO hot isostatic press. Reduced samples with high T_c's were also obtained by annealing in an argon atmosphere at 500 °C to serve as references in the neutron-diffraction study.

X-ray-diffraction studies confirmed the samples to be single phase. The x-ray-diffraction data were also used for determining the lattice parameters. The lattice parameters of the present samples are slightly different from those of the previous samples.[5,7,17] We believe this is due to the slight difference in cation compositions, most likely Cu substitution for the Tl site in $Tl_2Ba_2CuO_{6+\delta}$ (Ref. 17) and Tl substitution for the Ca site in $TlSr_2CaCu_2O_{7-\delta}$,[18] which are sensitive to synthesis conditions. Since the cation compositions do not change during the annealing process, we focused attention on relative changes in lattice parameters. The relative changes in lattice parameters, $\Delta a/a_0$ and $\Delta c/c_0$, were defined as the changes from the values for the samples annealed in 1 atm oxygen.

Superconductivity for the superconducting samples was confirmed by measurements of resistivity and diamagnetism. The resistivity was measured by the conventional four-point probe method. Dc susceptibility was measured by a superconducting quantum interference device magnetometer under a magnetic field of 10 Oe. The superconducting transition temperatures of the samples were defined as the temperature of the zero resistivity and the onset of the diamagnetic signal.

Neutron-diffraction measurements were performed in order to determine the precise crystal structures including site occupancies for the oxygen sites. Time-of-flight neutron-diffraction data were obtained at the Special Environment Powder Diffractometer (SEPD) at Argonne's Intense Pulsed Neutron Source (IPNS).[19] The crystal structures of $Tl_2Ba_2CuO_{6+\delta}$ and $TlSr_2CaCu_2O_{7-\delta}$ were refined by the Rietveld technique[20] using the high-resolution backscattered data with structural models based on the tetragonal space groups $I4/mmm$ (Ref. 21) and $P4/mmm$,[18] respectively. In the course of the refinements, large anisotropic thermal parameters were observed for the O(3) site in the TlO layer in $Tl_2Ba_2CuO_{6+\delta}$ and the Tl site in $TlSr_2CaCu_2O_{7-\delta}$ suggesting static displacements of the atoms, so these sites were assigned to positions displaced from their ideal positions with isotropic thermal parameters. (Refinements are not stable if anisotropic thermal parameters are assigned to sites that are statically displaced from ideal positions, as is done here.) The thermal parameters for the Sr and Ca sites in $TlSr_2CaCu_2O_{7-\delta}$ were found to be almost isotropic. The thermal parameter for the interstitial O(4) site in $Tl_2Ba_2CuO_{6+\delta}$ was fixed at 1.00 Å^2 because refinement is difficult due to its small occupancy.

The amount of incorporated oxygen was also confirmed by weight changes in samples annealed between in 1 atm oxygen and in high-pressure oxygen. Details of the experimental procedure were described in a previous paper.[5] Small increases in weight for the samples annealed in high-pressure oxygen corresponded to an oxygen incorporation of 0.02–0.04 atoms per each formula unit.

Transport properties were examined by resistivity and Hall coefficient measurements by the van der Pauw method using a disk sample of about 10 mm $\phi\times 0.3$ mm thick. The Hall coefficient was measured under a magnetic field of 8 T. The data for the samples annealed in 1 atm oxygen and in high-pressure oxygen were obtained using the same pellet.

III. RESULTS AND DISCUSSION

Rietveld refinements of the neutron-diffraction data for $Tl_2Ba_2CuO_{6+\delta}$ showed that the Tl site and the oxygen

TABLE I. T_c and refined structural parameters for the $Tl_2Ba_2CuO_{6+\delta}$ samples reduced in argon, annealed in 1 atm oxygen, and annealed in high-pressure oxygen. The atom positions are: Tl 4*e* (0,0,*z*), Ba 4*e* (0,0,*z*), Cu 2*b* (0,0,0.5), O(1) 4*c* (0,0.5,0), O(2) 4*e* (0,0,*z*), O(3) 16*n* (0,*y*,*z*), and O(4) 8*g* (0,0.5,*z*). The O(3) atom is assigned to a position displaced from the ideal position. Anisotropic thermal parameters are refined except for the O(3) and O(4) sites. B_{eq}, is the equivalent isotropic thermal parameter. The thermal parameter for the O(4) site is fixed at 1.00 (Å^2).

		Reduced in argon	Annealed in 1 atm oxygen	Annealed in high-pressure oxygen
	T_c (K)	60		
	a (Å)	3.867 26(3)	3.866 28(3)	3.867 12(2)
	c (Å)	23.234 0(3)	23.159 3(2)	23.148 3(2)
Tl:	z	0.297 05(6)	0.296 68(6)	0.296 63(6)
	B_{eq} (Å^2)	1.54	1.59	1.71
Ba:	z	0.083 42(9)	0.084 47(8)	0.084 85(8)
	B_{eq} (Å^2)	0.85	0.83	0.87
Cu:	B_{eq} (Å^2)	0.53	0.65	0.73
O(1):	B_{eq} (Å^2)	0.78	0.82	0.87
O(2):	z	0.382 92(7)	0.383 09(7)	0.383 13(7)
	B_{eq} (Å^2)	0.99	0.97	1.02
O(3):	y	0.089 6(7)	0.101 9(8)	0.105 0(8)
	z	0.210 7(7)	0.210 0(8)	0.209 6(8)
	B_{iso} (Å^2)	1.24(7)	2.20(8)	2.48(9)
O(4):	z	0.265 1	0.265 1(19)	0.265 4(14)
	n	0.026(10)	0.088(10)	0.118(11)
	B_{iso} (Å^2)	1.00	1.00	1.00
	R_{wp} (%)	5.343	5.244	4.766
	R_{exp} (%)	3.837	3.496	3.487

TABLE II. T_c and refined structural parameters for the $TlSr_2CaCu_2O_{7-\delta}$ samples reduced in argon, annealed in 1 atm oxygen, and annealed in high-pressure oxygen. The atom positions are Tl 4*m* (0,*y*,0.5), Sr 2*h* (0.5,0.5,*z*), Ca/Tl 1*c* (0.5,0.5,0), Cu 2*g* (0,0,*z*), O(1) 4*i* (0,0.5,*z*), O(2) 2*g* (0,0,*z*), and O(3) 1*d* (0.5,0.5,0.5). The Tl atom is assigned to a position displaced from the ideal position. Anisotropic thermal parameters are refined except for the Tl, Sr, and Ca sites. B_{eq} is the equivalent isotropic thermal parameter.

		Reduced in argon	Annealed in 1 atm oxygen	Annealed in high-pressure oxygen
	T_c (K)	65		
	a (Å)	3.793 95(2)	3.784 43(2)	3.783 31(2)
	c (Å)	12.128 08(11)	12.118 99(9)	12.120 41(9)
Tl:	y	0.082 9(6)	0.076 1(6)	0.076 4(6)
	B_{iso} (Å^2)	0.92(5)	0.86(4)	0.86(4)
Sr:	z	0.284 54(8)	0.287 78(8)	0.288 20(8)
	B_{iso} (Å^2)	0.84(2)	0.83(2)	0.86(2)
Ca/Tl:	n	0.80(1)/0.20(1)	0.81(1)/0.19(1)	0.79(1)/0.21(1)
	B_{iso} (Å^2)	0.57(4)	0.50(4)	0.56(4)
Cu:	z	0.136 68(8)	0.138 39(8)	0.138 66(8)
	B_{eq} (Å^2)	0.42	0.42	0.42
O(1):	z	0.129 41(7)	0.129 15(7)	0.129 12(7)
	B_{eq} (Å^2)	0.84	0.86	0.89
O(2):	z	0.334 4(1)	0.333 1(1)	0.332 9(1)
	B_{eq} (Å^2)	1.32	1.16	1.15
O(3):	n	0.862(9)	0.934(9)	0.966(10)
	B_{eq} (Å^2)	2.20	2.42	2.34
	R_{wp} (%)	4.647	4.696	4.705
	R_{exp} (%)	3.312	3.207	3.313

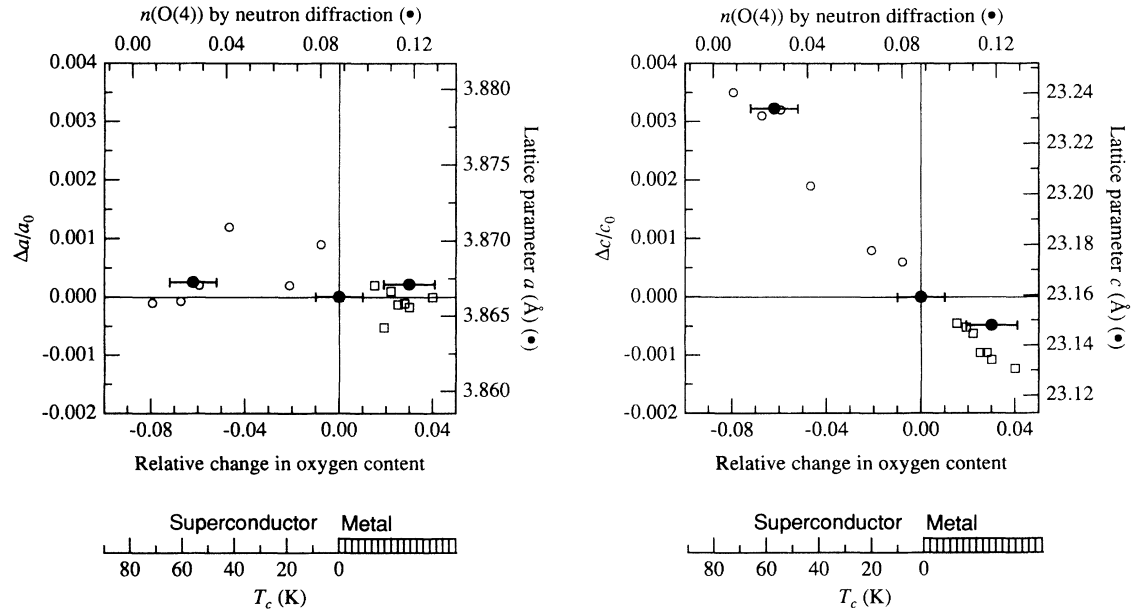

FIG. 1. Relative changes in lattice parameters a and c plotted vs relative changes in oxygen content for the $Tl_2Ba_2CuO_{6+\delta}$ samples. Data plotted as open symbols are obtained from x-ray-diffraction measurements and the relative changes in oxygen content are determined from weight measurements. Data plotted as closed symbols are obtained from neutron-diffraction measurements and the relative changes in oxygen content are determined from the refined occupation numbers for oxygen atoms. The origin of these relative changes is defined as the value for the samples annealed in 1 atm oxygen. Changes in the occupancy of the excess O(4) site and the lattice parameters determined by structural refinements of neutron-diffraction data for the measured three samples (closed symbols) are also seen in the upper and right axes, respectively. Since absolute values of lattice parameters measured by neutron and x-ray-diffraction do not agree (see text), x-ray results are plotted vs the relative change in lattice parameter. Data plotted as open circles are obtained from Refs. 5 and 17; open squares are from the present x-ray measurements. Corresponding T_c changes are shown in the lower part of the graph. This scale is an approximation of T_c derived from the almost linear relation between the relative change in oxygen content and T_c in Refs. 5 and 17.

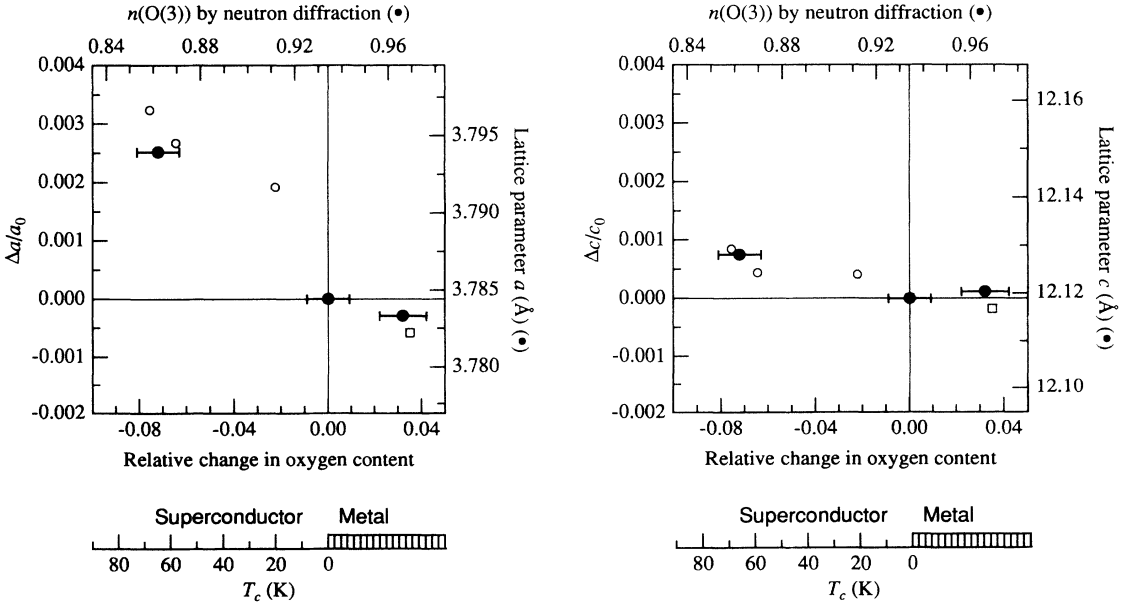

FIG. 2. Relative changes in lattice parameters a and c plotted vs relative changes in oxygen content for the $TlSr_2CaCu_2O_{7-\delta}$ samples. Format is the same as for Fig. 1. Changes in the occupancy of the deficient O(3) site are seen in the upper axes. Data plotted as open circles and the almost linear relation between the relative change in oxygen content and T_c are obtained from Refs. 7.

site O(3) in the TlO layer are fully occupied. Excess oxygen atoms located at an interstitial site O(4) between the double TlO layers are detected in the oxygenated and high-pressure oxygen-annealed $Tl_2Ba_2CuO_{6+\delta}$ samples. In $TlSr_2CaCu_2O_{7-\delta}$, the Tl site is fully occupied, but the oxygen site O(3) in the single TlO layer is deficient. About 20% of the Ca site is substituted by Tl. This is consistent with the 15–20% Ca deficient and Tl-rich starting composition (typically, Tl:Sr:Ca:Cu $=1.5:2.0:0.8:2.0$), which is necessary to obtain a single phase sample. No oxygen is seen in the Ca layer, even for the high-pressure oxygen-annealed $TlSr_2CaCu_2O_{7-\delta}$ samples. All such features in $Tl_2Ba_2CuO_{6+\delta}$ and $TlSr_2CaCu_2O_{7-\delta}$ agree well with the previous results of neutron-diffraction studies.[18,21]

Tables I and II show the results of Rietveld refinements for the $Tl_2Ba_2CuO_{6+\delta}$ and $TlSr_2CaCu_2O_{7-\delta}$ samples reduced in argon, annealed in 1 atm oxygen, and annealed in high-pressure oxygen. Changes of the occupancies of the excess oxygen site O(4) in $Tl_2Ba_2CuO_{6+\delta}$ and the deficient oxygen site O(3) in $TlSr_2CaCu_2O_{7-\delta}$ are clear. We conclude that the incorporation and release of oxygen atoms through the annealing process occurs at these sites. The most notable feature is the increased site occupancies of these sites in the samples annealed in high-pressure oxygen, which clearly demonstrates the oxygen incorporation by the annealing process in high-pressure oxygen. The amounts of incorporated oxygen determined by the changes of the site occupancies in the structural refinements with neutron-diffraction data are about 0.03 atoms per formula unit for the high-pressure oxygen-annealed $Tl_2Ba_2CuO_{6+\delta}$ and $TlSr_2CaCu_2O_{7-\delta}$ samples. The increase of oxygen content in the high-pressure oxygen-annealed samples is also measured by the increased sample weight. From these findings, we conclude that these samples are overdoped metals that are further beyond the superconductor-metal phase boundary than previous samples annealed in 1 atm oxygen.

Figures 1 and 2 show the relationships between the lattice parameters and the oxygen contents for $Tl_2Ba_2CuO_{6+\delta}$ and $TlSr_2CaCu_2O_{7-\delta}$, respectively. The previous data for the superconducting samples[7,17] are shown as open circles. The systematically shorter c-axis length ($Tl_2Ba_2CuO_{6+\delta}$) and a-axis length ($TlSr_2CaCu_2O_{7-\delta}$) for the present high-pressure oxygen-annealed samples (open squares) confirm the compositional changes as determined by refinements of site occupancies and weight changes. The results of neutron-diffraction analysis (closed symbols) are also quite consistent with the results of x-ray study. The site occupancies of O(4) in $Tl_2Ba_2CuO_{6+\delta}$ and O(3) in $TlSr_2CaCu_2O_{7-\delta}$ determined by neutron-diffraction study are also seen in the upper part of the figures. The lattice parameters of the high-pressure oxygen-annealed samples and the superconducting samples show the same linear correlations with oxygen doping, especially, the c-axis length in $Tl_2Ba_2CuO_{6+\delta}$ and a-axis length in $TlSr_2CaCu_2O_{7-\delta}$. Thus, the lattice parameters change continuously and systematically with oxygen doping from high-T_c superconductors to overdoped metals beyond the superconductor-metal phase boundaries with no evidence for a singularity at the boundary.

Figure 3 shows the temperature dependence of the resistivity and the Hall coefficient for the $Tl_2Ba_2CuO_{6+\delta}$

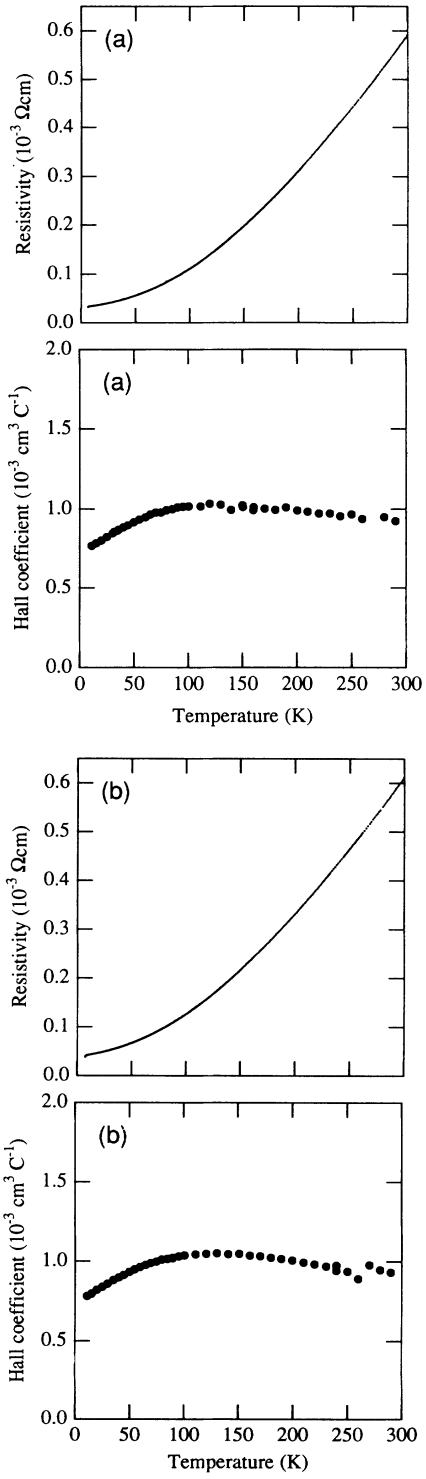

FIG. 3. Temperature dependence of the resistivity and the Hall coefficient for the $Tl_2Ba_2CuO_{6+\delta}$ samples annealed (a) in 1 atm oxygen and (b) in high-pressure oxygen.

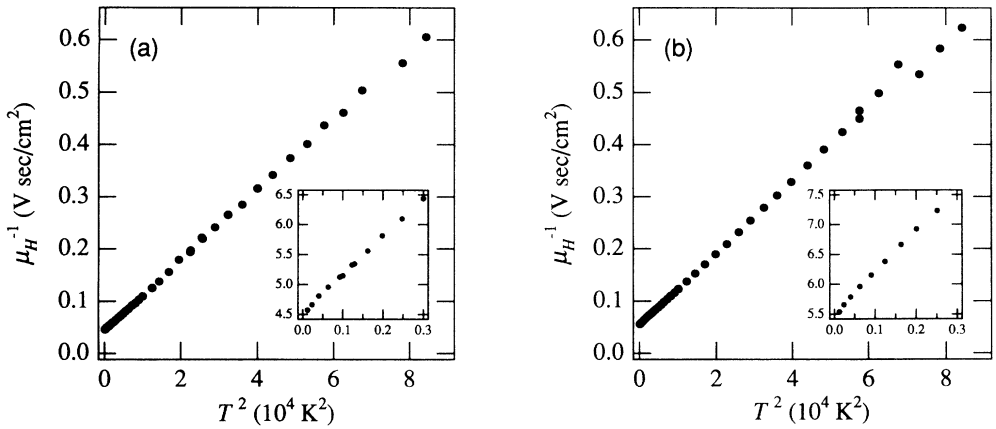

FIG. 4. Inverse Hall mobility, μ_H^{-1}, plotted vs T^2 for the $Tl_2Ba_2CuO_{6+\delta}$ samples annealed (a) in 1 atm oxygen and (b) in high-pressure oxygen.

samples annealed in 1 atm oxygen and in high-pressure oxygen. There is no significant difference in either the resistivity or the Hall coefficient for the two samples. The temperature dependence of the resistivity for the two samples can be fitted to a simple power expansion of $\rho=\rho_0+AT^{1.7}$ for the temperature range from 5 to 300 K. The temperature dependence of the Hall coefficient shows a characteristic maximum at around 120 K, which is the same feature observed in the superconducting samples.[6,15] Figure 4 shows the inverse Hall mobility $\mu_H^{-1}=\rho/R_H$ plotted against T^2. Clear correlations of $\mu_H^{-1}\propto T^2$ are observed for both the samples annealed in 1 atm oxygen and in high-pressure oxygen. This T^2 dependence of the inverse Hall mobility is exactly the same as that observed in superconducting $Tl_2Ba_2CuO_{6+\delta}$ samples.[14,15] This fact strongly suggests that the scattering mechanism that controls the transport properties in the present overdoped samples, which are beyond the superconductor-metal phase boundary, is the same as that for the superconducting materials. In other words, the electronic structures of both the superconducting and the overdoped metallic samples are essentially the same and a single $\sim T^2$ scattering mechanism governs the transport properties over the whole region.

It is worth noting that the Hall coefficient for the overdoped metallic sample remains positive. Figure 5 shows the change of the Hall coefficient of $Tl_2Ba_2CuO_{6+\delta}$ as a function of oxygen content, i.e., doping level. The Hall coefficient decreases gradually with doping and almost saturates in the overdoped metallic region. There is no singularity at the superconductor-metal phase boundary. This result is in sharp contrast with that for the $(La_{1-x}Sr_x)_2CuO_4$ system, where the Hall coefficient changes its sign near the boundary. Thus, the coincidence of the superconductor-metal phase boundary with the point of sign change in the Hall coefficient in the $(La_{1-x}Sr_x)_2CuO_4$ system may be accidental.

The saturation of the Hall coefficient in the overdoped metallic region deserves comment. In the overdoped region, as pointed out in the studies of $(La_{1-x}Sr_x)_2CuO_4$ (Ref. 1) and $Tl_2Ba_2CuO_{6+\delta}$,[6] the doping level based on the chemical composition does not correspond with the number of carriers determined from the Hall coefficient measurements. Since the Hall coefficient reflects the number of carriers that contributes to the transport properties, this observation might indicate that the hole concentration in the CuO_2 plane does not change significantly in the metallic region as "doping" is increased further. The hole carriers created by the additional oxygen incorporation may not be transferred to the CuO_2 planes but, rather, may be localized in the TlO charge reservoir layers. This means that the electronic structure of the high-pressure oxygen-annealed sample, which is clearly "further overdoped by oxygen" beyond the superconductor-metal phase boundary might still be

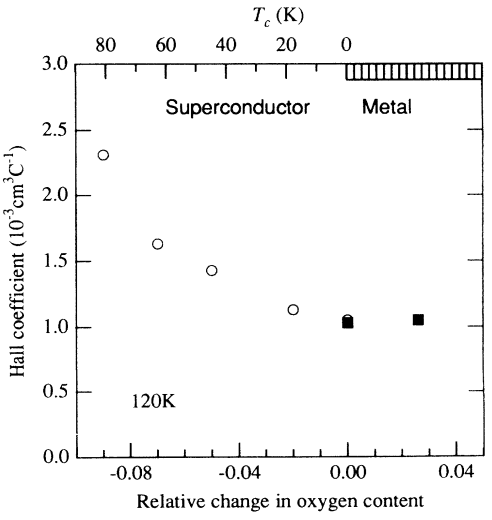

FIG. 5. Hall coefficient at 120 K plotted vs relative changes in oxygen content for $Tl_2Ba_2CuO_{6+\delta}$. Corresponding T_c changes are seen in the upper axis. Data plotted as closed symbols are obtained in the present experiments; data plotted as open symbols are from Ref. 6.

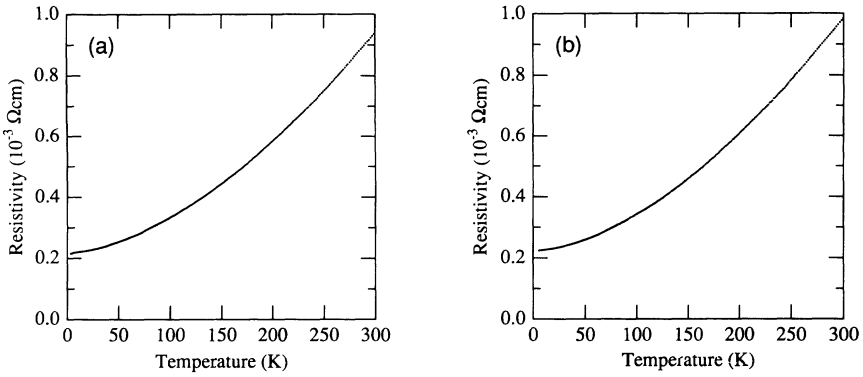

FIG. 6. Temperature dependence of the resistivity for the $TlSr_2CaCu_2O_{7-\delta}$ samples annealed (a) in 1 atm oxygen and (b) in high-pressure oxygen.

near the superconductor-metal phase boundary.

Similar results are obtained for the $TlSr_2CaCu_2O_{7-\delta}$ system. There is no significant change in the temperature dependence of the resistivity for the samples annealed in 1 atm oxygen and in high-pressure oxygen as shown in Fig. 6. The temperature dependencies for the two samples are almost $T^{1.7}$ for the temperature range from 5 to 300 K suggesting no drastic change in the electronic structure at the superconductor-metal phase boundary.

In conclusion, the present experimental results on overdoped $Tl_2Ba_2CuO_{6+\delta}$ and $TlSr_2CaCu_2O_{7-\delta}$ compounds show no singularity at the superconductor-metal phase boundary in either the crystal structure or the transport properties. In particular, the positive Hall coefficient and the T^2 dependence of the inverse Hall mobility in the overdoped Tl-based materials strongly suggest that the electronic structures are essentially the same as those of the corresponding superconducting materials. However, in contrast to the clear continuity of the crystal structural changes at crossing the superconductor-metal phase boundary, the "oxygen doping" beyond the boundary does not create additional itinerant hole carriers in the materials.

If we consider the T^2 dependence of the inverse Hall mobility and nearly T^2 dependence of the resistivity to be characteristic features of a two-dimensional Fermi liquid,[14] these results suggest that the electronic structure of the high-T_c superconductors should be described within this framework.

ACKNOWLEDGMENTS

This work was supported by the US Department of Energy, Division of Basic Energy Sciences-Materials Sciences, under Contract No. W-31-109-ENG-38, the National Science Foundation through the Science and Technology Center for Superconductivity under Grant No. DMR 91-20000, and NEC Corporation, Japan.

[1]H. Takagi, T. Ido, S. Ishibashi, M. Uota, S. Uchida, and Y. Tokura, Phys. Rev. B **40**, 2254 (1989).
[2]H. Takagi, R. J. Cava, M. Marezio, B. Battlog, J. J. Krajewski, and W. F. Peck, Jr., Phys. Rev. Lett. **68**, 3777 (1992).
[3]T. Nagano, Y. Tomioka, Y. Nakayama, K. Kishio, and K. Kitazawa, Phys. Rev. B **48**, 9689 (1993).
[4]P. G. Radaelli, D. G. Hinks, A. W. Mitchell, B. A. Hunter, J. L. Wagner, B. Dabrowski, K. G. Vandervoort, H. K. Viswanathan, and J. D. Jorgensen, Phys. Rev. B **49**, 4163 (1994).
[5]Y. Shimakawa, Y. Kubo, T. Manako, and H. Igarashi, Phys. Rev. B **40**, 11 400 (1989).
[6]Y. Kubo, Y. Shimakawa, T. Manako, and H. Igarashi, Phys. Rev. B **43**, 7875 (1991).
[7]Y. Kubo, T. Kondo, Y. Shimakawa, T. Manako, and H. Igarashi, Phys. Rev. B **45**, 5553 (1992).
[8]T. R. Chien, Z. Z. Wang, and N. P. Ong, Phys. Rev. Lett. **67**, 2088 (1991).
[9]J. M. Harris, Y. F. Yan, and N. P. Ong, Phys. Rev. B **46**, 14 293 (1992).
[10]W. Jiang, J. L. Peng, S. J. Hagen, and R. L. Greene, Phys. Rev. B **46**, 8694 (1992).
[11]A. Carrington, A. P. Mackenzie, C. T. Lin, and J. R. Cooper, Phys. Rev. Lett. **69**, 2855 (1992).
[12]G. Xiao, P. Xiong, and M. Z. Cieplak, Phys. Rev. B **46**, 8687 (1992).
[13]C. Kendziora, D. Mandrus, L. Mihaly, and L. Forro, Phys. Rev. B **46**, 14 297 (1992).
[14]Y. Kubo and T. Manako, Physica C **197**, 378 (1992).
[15]T. Manako, Y. Kubo, and Y. Shimakawa, Phys. Rev. B **46**, 11 019 (1992).
[16]P. S. Wang, J. C. Williams, K. D. D. Rathnayaka, B. D. Hennings, D. G. Naugle, and A. B. Kaiser, Phys. Rev. B **47**, 1119 (1993).
[17]Y. Shimakawa, Physica C **204**, 247 (1993).
[18]F. Izumi, T. Kondo, Y. Shimakawa, T. Manako, Y. Kubo, H. Igarashi, and H. Asano, Physica C **185-189**, 615 (1991).
[19]J. D. Jorgensen, J. Faber, Jr., J. M. Carpenter, R. K. Crawford, J. R. Haumann, R. L. Hitterman, R. Kleb, G. E. Ostrowski, F. J. Rotella, and T. G. Worlton, J. Appl. Crystallogr. **22**, 321 (1989).
[20]R. B. von Dreele, J. D. Jorgensen, and C. J. Windsor, J. Appl. Crystallogr. **15**, 581 (1982).
[21]Y. Shimakawa, Y. Kubo, T. Manako, H. Igarashi, F. Izumi, and H. Asano, Phys. Rev. B **42**, 10 165 (1990).